

Kinetic and Spectroscopic Characterization of Type II Isopentenyl Diphosphate Isomerase from *Thermus thermophilus*: Evidence for Formation of Substrate-Induced Flavin Species[†]

Steven C. Rothman, Travis R. Helm, and C. Dale Poulter*

Department of Chemistry, University of Utah, Salt Lake City, Utah 84112

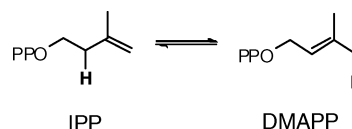
Received August 11, 2006; Revised Manuscript Received January 11, 2007

ABSTRACT: Type II isopentenyl diphosphate (IPP) isomerase catalyzes the interconversion of IPP and dimethylallyl diphosphate (DMAPP). Although the reactions catalyzed by the type II enzyme and the well-studied type I IPP isomerase are identical, the type II protein requires reduced flavin for activity. The chemical mechanism, including the role of flavin, has not been established for type II IPP isomerase. Recombinant type II IPP isomerase from *Thermus thermophilus* HB27 was purified by Ni²⁺ affinity chromatography. The aerobically purified enzyme was inactive until the flavin cofactor was reduced by NADPH or dithionite or photochemically. The inactive oxidized flavin–enzyme complex bound IPP in a Mg²⁺-dependent manner for which $K_D \sim K_m^{IPP}$, suggesting that the substrate binds to the inactive oxidized and active reduced forms of the protein with similar affinities. *N,N*-Dimethyl-2-amino-1-ethyl diphosphate (NIPP), a transition state analogue for the type I isomerase, competitively inhibits the type II enzyme, but with a much lower affinity. pH-dependent spectral changes indicate that the binding of IPP, DMAPP, and a saturated analogue isopentyl diphosphate promotes protonation of anionic reduced flavin. Electron paramagnetic resonance (EPR) and UV–visible spectroscopy show a substrate-dependent accumulation of the neutral flavin semiquinone during both the flavoenzyme reduction and reoxidation processes in the presence of IPP and related analogues. Redox potentials of IPP-bound enzyme indicate that the neutral semiquinone state of the flavin is stabilized thermodynamically relative to free FMN in solution.

Isopentenyl diphosphate (IPP)¹ isomerase catalyzes the interconversion of isopentenyl diphosphate and dimethylallyl diphosphate (DMAPP), the basic building blocks of isoprenoid molecules (Scheme 1). This family of natural products now consists of more than 35 000 compounds (1), which comprise several classes of biologically important molecules, including sterols, carotenoids, prenylated proteins, dolichols, heme A, and ubiquinones. IPP isomerase is essential in organisms that generate IPP through the mevalonate pathway found in eukaryotes, archaea, and some Gram-positive eubacteria (2). The enzyme, although not essential, is also found in most organisms that utilize the methylerythritol phosphate pathway, where isomerase activity is probably important for balancing the pools of IPP and DMAPP (3).

Two structurally unrelated forms of IPP isomerase have been identified. The type I enzyme resides in eukaryotes and in some eubacteria, while the type II protein is found in archaea and other eubacteria (4). Type I IPP isomerase was

Scheme 1: Interconversion of IPP and DMAPP



discovered more than 40 years ago and has been extensively characterized (5). The enzyme is a zinc metalloprotein (6) that catalyzes the isomerization of IPP and DMAPP by an antarafacial (7–9) protonation–deprotonation mechanism (10, 11). Structural studies and site-directed mutagenesis experiments have provided important information about how the substrate binds and have identified several active site residues essential for catalysis (12–14).

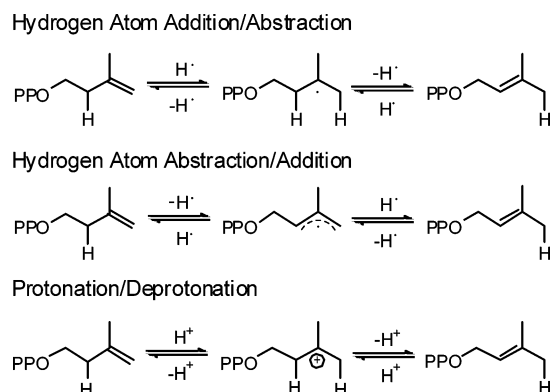
Type II IPP isomerase was first reported in 2001 (15). In contrast to the type I enzyme, type II isomerase requires flavin mononucleotide (FMN), a reducing agent, typically NADPH, and a divalent metal for activity. Presumably, NADPH is required to reduce the flavin to generate an active complex. Hemmi and co-workers (16) proposed a radical transfer mechanism for the isomerization reaction with the transient formation of a flavin semiquinone (Scheme 2), while others have suggested a structural role for the cofactor (4, 17) in a protonation–deprotonation mechanism similar to that of the type I enzyme. Type II IPP isomerase is an essential enzyme in *Streptococcus pneumoniae* and *Staphylococcus aureus*, both of which utilize the mevalonate route to isoprenoids. Since the type I enzyme is the exclusive IPP

[†] This work was supported by NIH Grant GM25521. S.C.R. was supported by NIH Postdoctoral Fellowship GM071114.

* To whom correspondence should be addressed. Telephone: (801) 581-6685. Fax: (801) 581-4391. E-mail: poulter@chemistry.utah.edu.

¹ Abbreviations: DMAPP, dimethylallyl diphosphate; ESI-MS, electrospray ionization mass spectrometry; FMN, flavin mononucleotide; FMN^{•−}, anionic reduced FMN; FMNH₂, reduced FMN; FMNH[•], FMN semiquinone; IPP, isopentenyl diphosphate; NIPP, *N,N*-dimethyl-2-amino-1-ethyl diphosphate; TCA, trichloroacetic acid; TEMPO, 2,2,6,6-tetramethylpiperidine 1-oxyl.

Scheme 2: Proposed Mechanisms for the Isomerization Reaction Catalyzed by Type II IPP Isomerase



isomerase in eukaryotes, the type II protein represents a logical target for antibacterial drugs (15). Our efforts to obtain a type II isomerase suitable for both mechanistic and structure–function studies led to the protein from *Thermus thermophilus*. We report the results of kinetic and spectroscopic studies that reveal a ligand-induced change in the state of flavin in the resting enzyme•FMN[−] complex upon binding IPP, DMAPP, isopentyl diphosphate, or NIPP.

EXPERIMENTAL PROCEDURES

Materials. IPP and isopentyl diphosphate were synthesized from their corresponding alcohols following the procedure of Davisson et al. (18). NIPP was prepared from 2-dimethylaminoethyl chloride as described previously (10). DMAPP was provided by W. Gao and N. Heaps. [¹⁴C]IPP was purchased from GE Healthcare (formerly Amersham Biosciences). The gene encoding *T. thermophilus* type II IPP isomerase (locus, TT_P0067) was previously cloned from *T. thermophilus* HB27 genomic DNA (19). Type II isomerase was expressed in *Escherichia coli* and purified as described previously (19), with the modification that DTT was excluded from the dialysis buffer. Additional modifications were applied for the protein purified for use in spectral assays. Riboflavin (200 μg/mL) was added to the expression media, and the purified protein was concentrated to ~1 mM with an Amicon Ultra-15 30K device (Millipore) and then dialyzed against 10 mM Tris buffer (pH 8.0) containing 20% glycerol, prior to storage at −80 °C. Protein used for assays in D₂O was dialyzed in a corresponding D₂O buffer. Glycerol, HEPES, Tris, and guanidinium•HCl were from USB Corp. D₂O was purchased from Cambridge Isotopes. Other reagents, unless specified, were purchased from Sigma.

Mass Spectrometry. Concentrated protein (10 μL) was diluted into 500 μL of a water/acetonitrile/formic acid mixture (80:20:0.2) and concentrated via ultrafiltration (Microcon YM-30, Millipore). The protein was resuspended in the same solution, concentrated, and resuspended in 250 μL of a water/acetonitrile/formic acid mixture (50:50:0.2) to give a final protein concentration of 15 μM. Positive ion ESI-MS was performed on a Waters Micromass Quattro II triple-quadrupole mass spectrometer.

Protein and Flavin Analysis. The concentration of the purified protein was determined by the BCA and Bradford protein assays (Pierce). The concentration of bound flavin was determined as follows. Protein (60 μL, ~6 mg/mL in 25 mM HEPES buffer at pH 7.5 and 25 °C) was mixed with

an equivalent volume of 10% TCA. The mixture was vortexed, placed on ice for ~2 min, and then centrifuged (2 min at 14000g and 4 °C). The supernatant was neutralized with an equal volume of 1 M Na₂HPO₄. Alternatively, protein was diluted to 1–2 mg/mL with 6 M guanidinium•HCl and 50 mM HEPES buffer (pH 7.5) and incubated for 30 min at room temperature. Flavin and protein were separated by ultrafiltration (Microcon YM-30, Millipore, 12 min, 14000g, 4 °C). As a control, a sample of protein-free FMN was carried through the identical procedure. Absorption spectra were measured with an Agilent 8453 diode array spectrophotometer. LC–MS analyses of guanidine-denatured samples were performed with a Waters Alliance 2695 HPLC system connected to a Micromass Quattro II triple-quadrupole mass spectrometer. Samples were chromatographed on a Phenomenex Prodigy ODS column, loaded and eluted with a 5 mM ammonium acetate (pH 6.0)/methanol (90:10) mobile phase, and analyzed by negative ion ESI-MS.

IPP Isomerase Assays. Isomerase activity was measured via the acid lability method (20) with modifications similar to those described by Kaneda (15). The conditions for assays are provided in Table 1. Reactions were initiated by the addition of enzyme, diluted in 1 mg/mL BSA and 10 mM HEPES buffer (pH 7.6), to the assay cocktail. After 10 min, the reaction was quenched with 200 μL of a 4:1 methanol/HCl mixture and followed by a 10 min incubation at 37 °C. Organic soluble products were extracted with 1 mL of ligroine (boiling point of 90–110 °C, Fisher Scientific). Radioactivity in 500 μL of the extract was measured by liquid scintillation (Ultima Gold Cocktail, Perkin-Elmer). Assays were performed at less than 10% substrate conversion. Activity versus concentration data were fit with the Michaelis–Menten equation via nonlinear regression with Grafit 5.0 (Erithacus Software).

IPP Binding Assays. Ultrafiltration assays (500 μL) contained 0–20 μM enzyme, 1 μM [¹⁴C]IPP (59 μCi/μmol), and 100 mM HEPES buffer (pH 7.0) containing 100 mM KCl, 2 mM MgCl₂, 40 μM FMN, and 0.8% glycerol. The mixtures were incubated for 10 min at 37 °C and transferred to a Microcon YM-30 (Millipore) filter unit. Following an additional 5 min at 37 °C, the samples were quickly centrifuged (1.5 min at 7200g). Approximately 70 μL of the 500 μL sample passed through the membrane (30 kDa cutoff) during a typical spin. Scintillation counting was performed on 50 μL of the flow-through and 50 μL of the original sample. [E•IPP] was calculated from the difference between [IPP]_{total} and [IPP]_{free}. The values for [E•IPP] at different concentrations of enzyme were fit to eq 1 (21) to determine *K*_D^{IPP}. An offset parameter *C* was included in eq 1 to correct for a small observed adsorption of unbound IPP onto the membrane.

$$[E \cdot IPP] = \frac{1}{2} (K_D^{IPP} + [IPP]_t + [E]_t - ((K_D^{IPP} + [IPP]_t + [E]_t)^2 - 4[IPP]_t[E]_t)^{1/2}) + C \quad (1)$$

Dependence of IPP Binding and Isomerization on MgCl₂. Concentrated protein was dialyzed for 24 h at 4 °C against 10 mM Tris buffer (pH 7.5) containing 20% glycerol and 5% Chelex-100 (Bio-Rad Laboratories) to remove divalent

Table 1: Steady State Kinetic Parameters for Type II IPP Isomerases

| enzyme | IPP | | | FMN | NADPH | MgCl ₂ |
|-------------------------------------|---|------------------------------|---|------------------------------|------------------------------|------------------------------|
| | $k_{\text{cat}} (\times 10^2 \text{ s}^{-1})$ | $K_{\text{m}} (\mu\text{M})$ | $k_{\text{cat}}/K_{\text{m}} (\times 10^3 \mu\text{M}^{-1} \text{ s}^{-1})$ | $K_{\text{D}} (\mu\text{M})$ | $K_{\text{D}} (\mu\text{M})$ | $K_{\text{D}} (\mu\text{M})$ |
| <i>T. thermophilus</i> ^a | 17.9 ± 0.2 | 5.6 ± 0.3 | 32 | 4.69 ± 0.55 | 110 ± 10 | 130 ± 10 |
| <i>B. subtilis</i> ^b | 25 | 670 | nr ^d | nr ^d | nr ^d | nr ^d |
| <i>Synechocystis</i> ^c | 23 | 52 | 4.4 | nr ^d | nr ^d | nr ^d |

^a Assay conditions for IPP parameters were as follows: 200 mM HEPES (pH 7.0), 6–10 nM *T. thermophilus* type II IPP isomerase, 1–40 μM [¹⁴C]IPP (10–59 $\mu\text{Ci}/\mu\text{mol}$), 40 μM FMN, 2 mM NADPH, 2 mM MgCl₂, and 0.14 mg/mL BSA at 37 °C. ^b From ref 28; k_{cat} calculated from the reported V_{max} . ^c From ref 27. ^d Not reported.

metal. Assay buffers and reagents were mixed with 5% Chelex for 1 h at 25 °C and filtered. Plasticware used in assays was washed with H₂O that had been treated with Chelex and filtered. Assays were conducted at 0–10 mM MgCl₂. The data were fit with the Michaelis–Menten equation to calculate $K_{\text{D}}^{\text{MgCl}_2}$. Ultrafiltration assays were used to determine the effect of Mg²⁺ on binding of IPP to the E•FMN_{ox} complex. Microcon YM-30 (Millipore) filtration units were incubated with 200 mM EDTA, centrifuged, and then rinsed twice with Chelex-treated water. Assays were performed as described above with 1 μM [¹⁴C]IPP (59 $\mu\text{Ci}/\mu\text{mol}$), 0 or 12 μM Chelex-treated enzyme, and 0 or 2 mM MgCl₂. MgCl₂ did not alter the small amount of IPP absorbed on the membrane observed in the absence of protein. In a second experiment, 1 mM EDTA with either 0 or 5 mM MgCl₂ was employed instead of Chelex. K_{D} in the presence of 1 mM EDTA without MgCl₂ was measured as described above.

Spectroscopic Assays with NADPH. Anaerobic assays used 800 μL reaction mixtures in 200 mM HEPES buffer (pH 7.0) containing 25 μM enzyme-bound FMN and 10 mM MgCl₂ at 37 °C. The mixtures were placed in a cuvette sealed with a silicone septum and purged with nitrogen. NADPH (2 mM) and then 50 μM IPP were added anaerobically via airtight syringes.

Photochemical Spectroscopic Assays. Photoreduction was performed in a 3.5 mL gastight all-glass cuvette (Starna Cells) with two side arms (one with a stopcock) and a three-way stopcock. Joints and stopcocks were sealed with Apiezon N high-vacuum grease. The cuvette chamber contained 2.1 mL (final concentrations are indicated for 2.2 mL after mixing) of 100 mM HEPES buffer (pH 7.0 or 8.5) containing 100 mM (pH 7.0) or 40 mM (pH 8.5) KCl, 20 μM enzyme-bound FMN (30–40 μM total enzyme), 5 μM added FMN, 2.25 μM riboflavin, 5% glycerol, 2 mM MgCl₂, and 1 mM sodium oxalate at 37 °C. The substrate side arm contained 100 μL of 50 mM HEPES buffer (pH 7.0 or 8.5) containing 55 μM (final concentration at pH 7.0) or 200 μM (final concentration at pH 8.5) IPP, 5.5 μM riboflavin, and 1 mM sodium oxalate at 37 °C. The final IPP concentration was saturating at each pH. Related experiments were conducted with NIPP at pH 7.0 (250 μM) and pH 8.5 (1 mM) and isopentyl diphosphate at pH 7.0 (10 mM). The side arm with the stopcock was filled with 1 mL of 100 mM Tris buffer (pH 8) containing 1 mM methyl viologen, 3 μM proflavine hemisulfate, and 10 mM EDTA. Six to eight cycles of degassing under vacuum and repressurization with OxiClear (LabClear) purified argon were performed before the cuvette was sealed. The samples were photoreduced by irradiation with a 300 W slide projector. To minimize oxygen contamination, the side arm containing methyl viologen was pho-

toreduced and allowed to oxidize over time with shaking (22). This procedure was conducted three times over a 20–30 min period. The side arm with the substrate was also photoirradiated briefly. Photoreduction of the main solution, prior to or after mixing with substrate, was achieved within 15 min of photoirradiation as determined from spectra taken at ~1 min intervals. The spectrum of the enzyme/substrate mixture was monitored over time at 37 °C with an Agilent 8453 diode array spectrophotometer.

EPR Spectroscopy. Reactions for EPR spectroscopy were performed in a Coy Labs anaerobic chamber. Samples and buffers were purged with purified argon before being placed in the glovebox. To generate the flavin semiquinone, 5 μL of 50 mM sodium dithionite in 50 mM Tris buffer (pH 8.7) was added to a 250 μL mixture of 200 mM HEPES buffer (pH 7.7 or 7.2) containing 2 mM MgCl₂, 3–10% glycerol, 100 μM enzyme-bound FMN, and either 250 μM IPP, 250 μM DMAPP, or 10 mM isopentyl diphosphate.

Reactions in D₂O were performed in a similar manner at pD 7.7 with buffers and enzyme prepared in or dialyzed against D₂O. Following reduction, samples were quickly transferred to an EPR tube with a rubber septum, removed from the glove box, and frozen in liquid nitrogen. In an attempt to detect a substrate radical–flavin radical pair, 6.25 μL of 200 mM sodium dithionite was first added to a mixture containing 400 μM enzyme-bound FMN without substrate. After an ~2 min incubation to ensure complete flavin reduction, the substrate was added to the mixture and treated as described above. Continuous wave EPR spectra were obtained at 77 K with a Bruker ESP300 spectrophotometer operating at X-band frequencies. Conditions for measurement are provided in Figure 4. TEMPO (50 μM) in a methanol/H₂O mixture (98:2) was employed as a standard for calculation of g factors (23).

Redox Potentiometry. Redox titrations were carried out in a glass anaerobic cuvette similar to the apparatus described by Dutton (24). This device was fitted with a silicone stopper containing a reference silver/silver chloride electrode in 3 M NaCl and a platinum measuring electrode. The cuvette chamber contained 7 mL of degassed 200 mM HEPES buffer (pH 8.0) containing 2 mM MgCl₂, 150 μM IPP, and 30–60 μM redox mediator at 25 °C. The redox mediator dyes used for the titrations were as follows: neutral red ($E_{\text{m}} = -325$ mV), anthraquinone 2-sulfonate ($E_{\text{m}} = -225$ mV), 2-hydroxy-1,4-naphthoquinone ($E_{\text{m}} = -152$ mV), 2,5-dihydroxy-*p*-benzoquinone ($E_{\text{m}} = -60$ mV), menadione ($E_{\text{m}} = 0$ mV), and phenazine ethosulfate ($E_{\text{m}} = 55$ mV). Purified argon was bubbled into the solution for 3–4 h. Enzyme (25 μM final) was added via syringe, and the solution was further deoxygenated over the course of 1–3 h. Reductive titrations were performed with 3 mM

sodium dithionite and oxidative titrations with 24 mM potassium ferricyanide. Once the voltage reading stabilized at each titration point, absorption spectra were monitored with an Agilent 8453 diode array spectrophotometer. Changes in absorbance at 620 nm, representing the neutral semiquinone, were plotted as a function of the ambient redox potential. Data were fit using a Nernst function describing a one-electron redox process. The calculated midpoint redox potentials were corrected for the potential of the Ag/AgCl reference electrode by adding 209 mV.

RESULTS

Mass Spectrometry and Flavin Content. Type II IPP isomerase from *T. thermophilus* bearing an N-terminal His₆ tag was expressed in *E. coli* and purified in two steps via heat treatment followed by Ni-NTA chromatography (19). The protein maintained a yellow color throughout purification, consistent with retention of bound flavin. A sample of protein prepared for ESI-MS was colorless and gave an observed mass of $38\,098 \pm 0.01\%$ Da. This value agrees with the calculated mass of 38 100 Da for the recombinant apoenzyme with the N-terminal His₆ tag and a factor Xa protease site.

The protein was denatured by treatment with 5% trichloroacetic acid (TCA) followed by centrifugation or by treatment with 6 M guanidinium hydrochloride, and then by ultrafiltration, to release the bound flavin and separate the cofactor from the protein. Both methods yielded similar quantities of free flavin, as determined by UV-vis spectroscopy. Spectra of free and enzyme-bound cofactor at equal-molar concentrations are shown in Figure 1. Free flavin has absorbance maxima at 374 and 446 nm, consistent with the reported spectrum of FMN (25). LC-MS of the denatured samples gave a peak at m/z 455 for FMN, while the fluorescence properties of the guanidinium-released cofactor closely resemble those of free FMN (see the Supporting Information). The absorption maxima shift to 368 and 460 nm, respectively, with a slight decrease in intensity in the enzyme-FMN complex. On the basis of a comparison of spectra for bound and released or free FMN ($\epsilon_{445} = 12\,500\text{ M}^{-1}\text{ cm}^{-1}$), an extinction coefficient of $11\,300\text{ M}^{-1}\text{ cm}^{-1}$ at 460 nm was calculated for the enzyme-FMN complex with an FMN occupancy of 32 or 25%, employing the BCA or Bradford assay, respectively. Supplementation of expression media with 200 $\mu\text{g/mL}$ riboflavin

increased the occupancy to 70%. The activity of purified enzyme was also enhanced by addition of exogenous FMN. A plot of v/E_T versus [FMN] was hyperbolic with a half-maximal increase in rate at $\sim 5\text{ }\mu\text{M}$ FMN (see the Supporting Information). Assuming that the maximal rate reflects saturation of IPP isomerase by FMN, the 2.9-fold increase in the rate at 37 °C is consistent with a predicted increase of 3.1-fold, corresponding to 32% occupancy determined for the purified protein by the spectral analyses described above and the BCA protein assay. The increase in activity upon preincubation of the enzyme with 250 nM FMN during time course measurements indicated slow tight binding of the cofactor (see the Supporting Information). The data were fit to a pseudo-first-order equation to give a k_{obs} of $(1.0 \pm 0.2) \times 10^{-3}\text{ s}^{-1}$, which provides an approximate k_{on} near $10^4\text{ M}^{-1}\text{ s}^{-1}$ for addition of FMN to the type II protein at 37 °C.

IPP Binding and Isomerization. The steady state kinetic constants for the conversion of IPP to DMAPP were determined under aerobic conditions at 37 °C (Table 1). Preincubation of the enzyme for 1 h at 37 °C prior to the addition of substrate did not result in a loss of enzyme activity. While the activity of the enzyme is higher at 60 °C, 37 °C was used in our studies to minimize fluctuations in temperature, minimize changes in concentration due to condensation of water on the sides of the cuvettes, and increase the stability of the enzyme. The affinity of radio-labeled IPP for the enzyme-FMN complex was measured at 37 °C using an ultrafiltration binding assay, where $K_{\text{D}}^{\text{IPP}} = 4.4 \pm 0.4\text{ }\mu\text{M}$ (see the Supporting Information). This value is similar to the $K_{\text{M}}^{\text{IPP}}$ determined under steady state conditions. NIPP, a potent transition state analogue/slow tight-binding inhibitor for type I IPP isomerase ($K_{\text{D}} < 0.12\text{ nM}$) (10), was evaluated as an inhibitor of the type II enzyme. Under steady state conditions, NIPP was a competitive inhibitor with a $K_{\text{I}}^{\text{NIPP}}$ of $5.1 \pm 0.5\text{ }\mu\text{M}$ at 37 °C (see the Supporting Information). Time-dependent inhibition of NADPH-reduced enzyme by 6 μM NIPP was not observed following a 40 min incubation prior to IPP addition (data not shown). Isopentyl diphosphate, a saturated analogue of IPP and DMAPP, inhibited turnover of 5 μM IPP ($\text{IC}_{50} = 1.2 \pm 0.1\text{ mM}$).

Catalytic Requirement for Reduced FMN. Type II IPP isomerase, when purified and assayed under aerobic conditions, needs a reducing agent for activity (4, 15, 26–29). The oxidized form of the *T. thermophilus* enzyme was also inactive. An apparent $K_{\text{D}}^{\text{NADPH}}$ value of $110 \pm 10\text{ }\mu\text{M}$ was measured under aerobic conditions (Table 1). Spectroscopic assays (described in the next section) show that enzyme-bound flavin is rapidly reduced by NADPH. Sodium dithionite also reduces enzyme-bound FMN to FMNH[•] and can substitute for NADPH to produce an active enzyme. Under anaerobic conditions, the enzyme is also only active in the presence of a reducing agent (J. Johnston, unpublished observations).

Mg²⁺ Dependence for Catalysis and Binding. The requirement of Mg²⁺ for catalysis and for substrate binding was evaluated. When purified IPP isomerase was assayed in a metal-free buffer, the enzyme had $\sim 20\%$ of the activity observed in buffer containing 2 mM MgCl₂. The activity decreased to $< 0.2\%$ when the protein was dialyzed against Chelex and assayed in Chelex-treated metal-free buffer. $K_{\text{D(IPP)}}^{\text{MgCl}_2} = 130 \pm 10\text{ }\mu\text{M}$ (see Table 1). In ultrafiltration

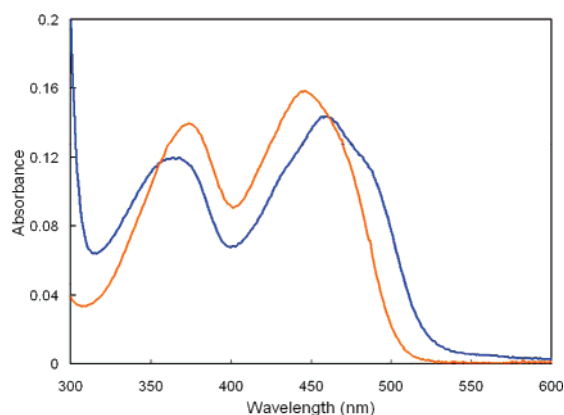


FIGURE 1: UV-visible spectra of enzyme-bound (dark blue) and 5% TCA-released (orange) FMN at equal concentrations.

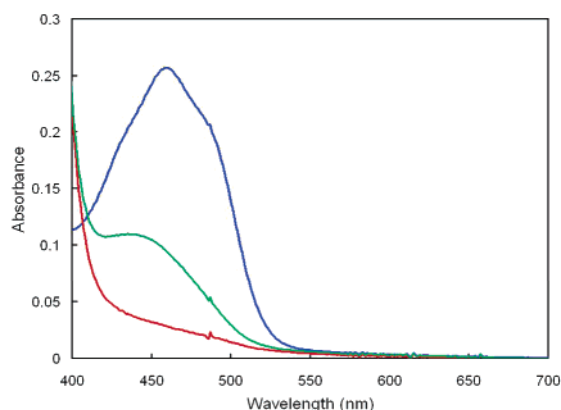


FIGURE 2: Reduction of enzyme-bound FMN by NADPH under anaerobic conditions at pH 7.0 and 37 °C. Shown are spectra of 25 μ M FMN in assay buffer (dark blue), FMN $^{\cdot-}$ formed immediately after mixing with 2 mM NADPH (red), and FMN $^{\cdot-}$ formed after the subsequent addition of 50 μ M IPP (dark green).

experiments, the fraction of radiolabeled IPP (1 μ M) bound to excess enzyme (12 μ M) increased from 0.08 to 0.7 when MgCl $_2$ was added to the assay buffer. A similar MgCl $_2$ enhancement of binding was also observed for the untreated enzyme (12 μ M) with 1 mM EDTA. A K_D of 84 ± 9 μ M was measured for the binding of IPP to the oxidized enzyme in the presence of 1 mM EDTA without MgCl $_2$ (data not shown).

Spectroscopic Analysis of Bound FMN and FMN $^{\cdot-}$. UV-visible spectroscopy was used to characterize the bound flavin species in enzyme•FMN and enzyme•FMN $^{\cdot-}$ complexes (25, 30). Under anaerobic conditions, the absorbance at 460 nm decreased rapidly upon mixing the enzyme•FMN complex and NADPH (Figure 2). This change was also observed under aerobic conditions. These results are consistent with reduction of the enzyme•FMN complex to the enzyme•FMN $^{\cdot-}$ complex. However, the spectra do not permit FMN $^{\cdot-}$ to be identified unambiguously because of the intense absorption for NADPH at 340 nm. To circumvent this problem, the flavin was reduced photochemically with oxalate under anaerobic conditions (31, 32). A time course for photoreduction of FMN in the presence of excess protein is shown in Figure 3a. The reaction proceeds to give a series of spectra with an isosbestic point at 330 nm, indicating that the reaction occurs without the accumulation of an intermediate. The final species has an absorbance maximum at 352 nm ($\epsilon \sim 5500$ M $^{-1}$ cm $^{-1}$) characteristic of anionic reduced FMN (Figure 3b), which has a peak at 342 nm when free in solution (25). FMN $^{\cdot-}$ is the typical protonation state for the reduced cofactor in most flavoenzymes (33). The photoreduced enzyme is enzymatically active (J, Johnston, unpublished results).

When IPP is added to the enzyme•FMN $^{\cdot-}$ complex obtained by photoreduction at pH 7.0, the UV-visible absorbance spectrum of the flavin gives a new spectrum with a peak at 426 nm ($\epsilon \sim 4300$ M $^{-1}$ cm $^{-1}$) and a shoulder at \sim 320 nm (Figure 3b). A similar change is seen in the 400–450 nm region when IPP is added to the enzyme•FMN $^{\cdot-}$ complex generated by reduction with NADPH (Figure 2). The absorption features for the complex resemble those reported for FMN $^{\cdot-}$ bound to *E. coli* thioredoxin reductase, where the N1 position of the flavin is protonated at a physiological pH (25, 34). In addition, the UV-visible

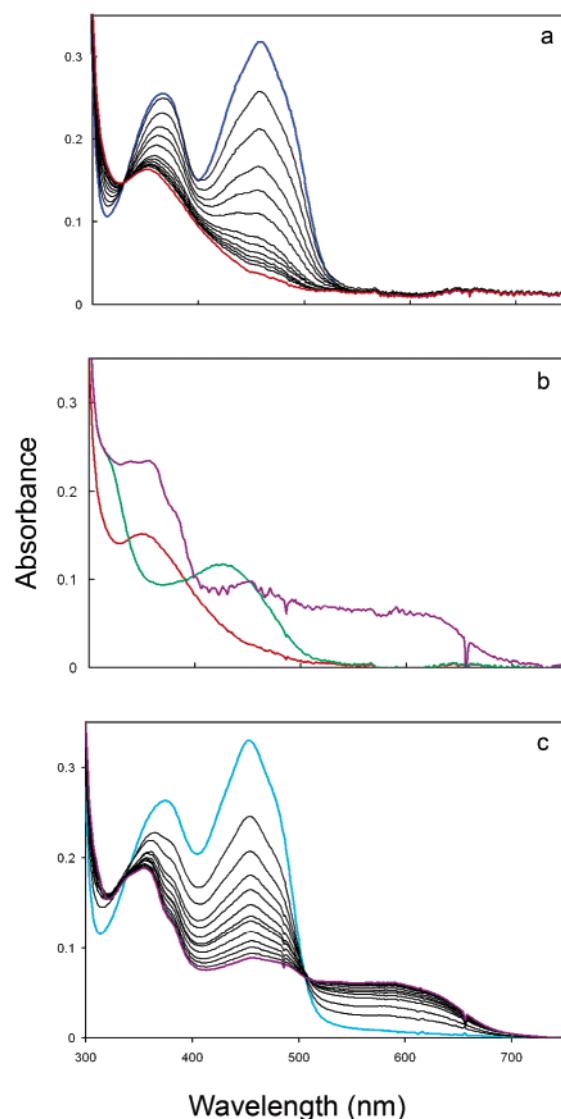


FIGURE 3: UV-visible spectra of isomerase•flavin complexes at pH 7.0 and 37 °C. (a) Time course for photoreduction of the enzyme•FMN complex (dark blue) to the enzyme•FMN $^{\cdot-}$ complex (red). (b) Enzyme•FMN $^{\cdot-}$ (red), enzyme•FMN $^{\cdot-}$ •IPP (dark green), and enzyme•FMN $^{\cdot-}$ •IPP (dark purple) complexes. (c) Time course for photoreduction of the oxidized enzyme•FMN•IPP complex (light blue) to the enzyme•FMN $^{\cdot-}$ •IPP complex (dark purple).

absorbance spectrum of neutral reduced flavin in a polar organic solvent is similar to those of the two flavoenzymes (25). These similarities suggest that the binding of IPP induces concomitant protonation of the flavin in the enzyme•FMN $^{\cdot-}$ complex at pH 7.0. When the pH of the buffer is increased from 7.0 to 8.5, the UV-visible spectrum of the enzyme•FMN $^{\cdot-}$ complex is essentially unaltered. In contrast, the spectrum of the isomerase•FMN $^{\cdot-}$ •IPP complex changed to one consistent with an isomerase•FMN $^{\cdot-}$ •IPP species (Figure 4a). The reduced enzyme bound to NIPP at either pH 7.0 or 8.5 exhibits a UV spectrum similar to that of the IPP complex at pH 8.5 (Figure 4b), consistent with stabilization of the anionic form of the reduced cofactor by the positive charge at N3 of NIPP. Isopentyl diphosphate elicited spectral changes consistent with flavin protonation (data not shown). The retention of a peak near 430 nm for

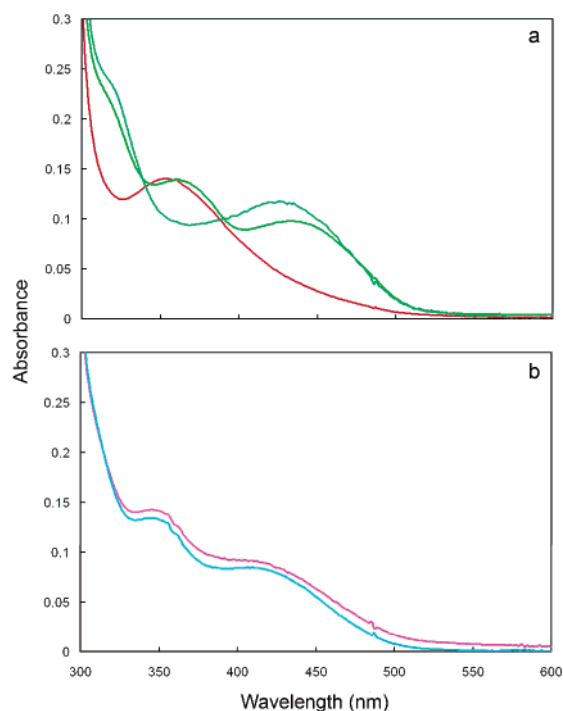


FIGURE 4: Effect of pH on the spectra of isomerase•flavin complexes at 37 °C. (a) Spectra of enzyme•FMNH[−] (red) and enzyme•FMNH₂•IPP (dark green) complexes at pH 7.0 and the enzyme•FMNH[−]•IPP complex (light green) at pH 8.5. (b) Spectra of the enzyme•FMNH[−]•NIPP complex at pH 7.0 (pink) and 8.5 (cyan).

each of the complexes at pH 8.5 may indicate substrate stabilization of a planar conformation for bound FMN (35).

Upon prolonged incubation in the presence of small amounts of residual oxygen, the enzyme•FMNH[−] complex slowly oxidizes to the enzyme•FMN complex without the formation of a detectable intermediate. In contrast, under similar conditions, the enzyme•FMNH₂•IPP complex is oxidized to an intermediate with an absorption at 550–650 nm (purple, Figure 3b). Although the absorption at 550–650 nm could represent a charge transfer complex, the accompanying intense peak near 350 nm indicates formation of the neutral flavin semiquinone (30, 36). The enzyme•FMNH[−]•IPP complex was stable to extended incubation in the sealed glass cuvette. The spectrum shifted to one characteristic of the enzyme•FMN•IPP complex only after the sample was fully exposed to atmospheric oxygen.

Oxidized enzyme•FMN and enzyme•FMN•IPP complexes give similar spectra (Figure 3a,c). Photoreduction of the enzyme•FMN complex cleanly generates the enzyme•FMNH[−] complex (Figure 3a). In contrast, photoreduction of the enzyme•FMN•IPP complex cleanly produces the enzyme•FMNH[−]•IPP complex (Figure 3c). An extended 40 min illumination failed to generate the spectrum for the enzyme•FMNH₂•IPP complex that was observed when IPP was added to the photoreduced enzyme•FMNH[−] complex.

EPR Spectroscopy of the Flavin Semiquinone. EPR spectroscopy was employed to evaluate the nature of the putative substrate-dependent flavin radical. Dithionite reduction of the enzyme•FMN•IPP complex initially produced the neutral semiquinone species observed during photoreduction (unpublished results). EPR spectra for the partially reduced complex at pH (or pD) 7.7 are shown in Figure 5. A strong signal was seen with a *g* factor of 2.0046 and a line width

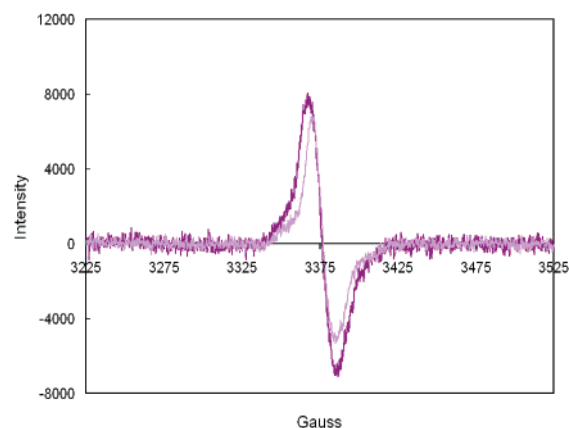


FIGURE 5: EPR spectra of the enzyme•FMNH[−]•DMAPP complex at 77 K produced by reduction (pH 7.7 and 25 °C) of the enzyme•FMN•DMAPP complex in H₂O (dark purple) and D₂O (light purple). Spectrometer settings were as follows: microwave frequency, 9.48 GHz; microwave power, 20 μ W; modulation frequency, 100 kHz; modulation amplitude, 1 G. The line widths are 19 G in H₂O and 15 G in D₂O. The *g* factor was 2.0046 based on a TEMPO standard.

of 19 G, which narrows to 15 G in D₂O. These features are consistent with the presence of a neutral flavin radical (37). Similar spectra were observed upon dithionite reduction of the IPP (pH 7.2 and 7.7) and isopentyl diphosphate complexes, but not for the enzyme•FMN complex. A signal for the flavin radical signal was also observed when the NADPH-reduced enzyme•FMNH₂•IPP complex was briefly exposed to oxygen. In an attempt to detect a substrate–flavin radical pair, 500 μ M IPP was added to fully reduced 400 μ M enzyme•FMNH[−] complex. Only faint EPR signals, similar to those seen for the enzyme•FMNH[−]•IPP complex generated by reduction of the flavin in the presence of IPP, were observed (data not shown). At this point, we cannot rule out the possibility of contamination of the sample by trace quantities of oxygen. In addition, a semiquinone signal was not observed via absorption spectroscopy when 250 μ M IPP was added anaerobically to 200 μ M enzyme•FMNH[−] complex.

Redox Potentiometry. Anaerobic redox titrations were performed to determine the midpoint redox potentials for enzyme-bound flavin in the presence of IPP. Oxidative and reductive titrations employing dye mediators were carried out at pH 8.0 and 25 °C. The spectra at each titration point were recorded (see the Supporting Information). The formation or loss of the neutral semiquinone, based on absorbance at 620 nm, was plotted as function of the ambient redox potential (Figure 6). A small 18 mV difference was observed for the oxidized flavin–semiquinone couple midpoint redox potentials in the two directions (part A), which probably results from incomplete equilibration before the measurements. There was no difference for the semiquinone–reduced flavin couple (part B). The measured midpoint redox potentials (*n* = 1) for the oxidized–neutral semiquinone (oxidative titration) and neutral semiquinone–reduced couples are -83 ± 1 and -196 ± 1 mV, respectively. These contrast with the redox potentials for free flavin at pH 8 of -364 mV for the oxidized–semiquinone couple and -119 mV for the semiquinone–reduced couple, calculated from the reported values (-301 and -101 mV, respectively) at pH 7 and 20 °C (38).

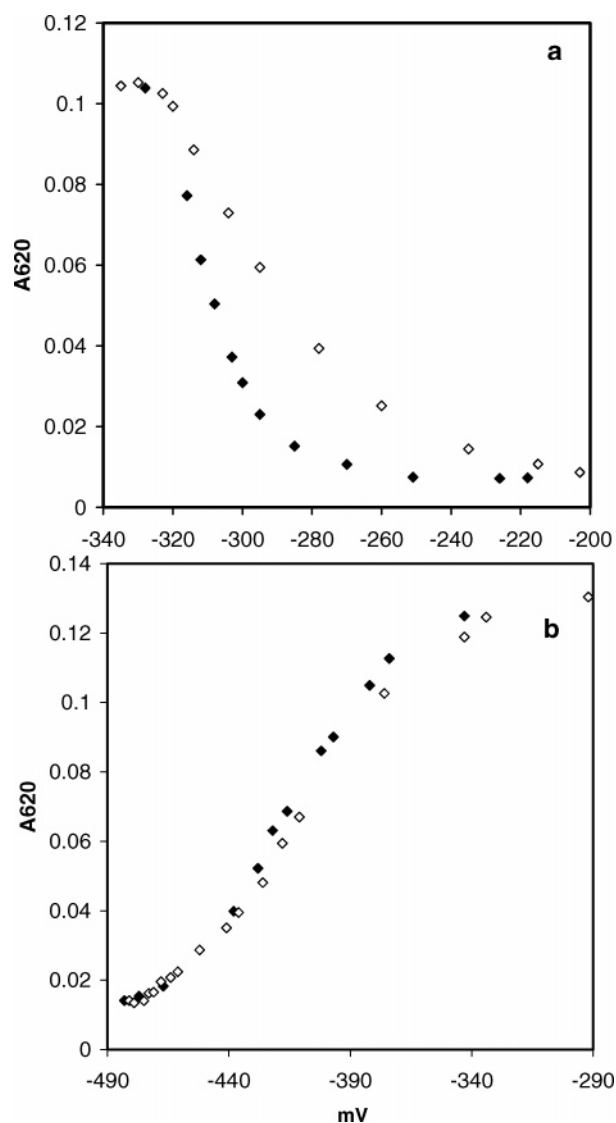


FIGURE 6: Changes in the enzyme•FMN•IPP complex oxidation state as a function of the ambient redox potential (pH 8.0 and 25 °C). Shown are the spectral changes associated with the interconversion of the oxidized and semiquinone states (a) and the semiquinone and reduced states (b). Titrations were performed reductively with sodium dithionite (◆) and oxidatively with potassium ferricyanide (◇).

DISCUSSION

As a prelude to work with type II IPP isomerase, we cloned and conducted preliminary experiments with the enzymes from *Synechocystis* sp. strain PCC 6803 (27), *Methanothermobacter thermautotrophicus* (26), *S. pneumoniae*, *Thermoplasma acidophilum*, and *T. thermophilus* HB27. Of these, the enzyme•FMN complex from *T. thermophilus* HB27 was soluble and stable, even when studied at higher temperatures, and that protein was selected for additional studies. As reported for other type II isomerases, the *T. thermophilus* enzyme catalyzed the isomerization of IPP to DMAPP in the presence of bound FMN, a reducing agent, and MgCl_2 . The value for k_{cat} at 37 °C (Table 1) was similar to those for mesophilic enzymes from *Bacillus subtilis* (28, 39) and *Synechocystis* sp. strain PCC 6803 (27) and increased ~10-fold at the optimal temperature near 60 °C (unpublished results). Freshly purified *T. thermophilus* type II IPP isomerase contained 0.3–0.7 equiv of FMN, depending on

the conditions employed for expression. Upon incubation with FMN, the protein binds additional cofactor in a slow tight binding process similar to that proposed for the type II isomerase from *Sulfolobus shibatae* (29).

Type II isomerase, typically purified in the presence of oxygen, gave an inactive enzyme containing oxidized flavin. Reduction of the cofactor with NADPH or dithionite was required to generate an active enzyme•reduced flavin complex (15, 16, 26, 28). Laupitz and co-workers (4) reported that *B. subtilis* type II isomerase purified from a recombinant *E. coli* strain under anaerobic conditions was active without addition of NADPH to the assay buffer. It is curious to note that they also reported that added FMN was required for activity in the anaerobic assay and that FMN was not reduced by NADPH in the presence of enzyme. We found that FMN in the *T. thermophilus* enzyme was rapidly reduced by NADPH or dithionite and was reduced photochemically to the fully reduced anion. The enzyme was active regardless of the method of reduction. Thus, FMNH^- is the form of the flavin cofactor in the resting state of the catalytically active enzyme.

Type II IPP isomerase requires a divalent metal, Mg^{2+} , Mn^{2+} , or Ca^{2+} , for activity (4, 15, 28). A specific role for the metal has not been established. The type I enzyme requires two divalent metals (13). Zn^{2+} is located in a hexacoordinate His_3Glu_2 binding site that is to be part of the catalytic machinery for protonation of the carbon–carbon double bond in IPP. The second metal, Mg^{2+} , helps anchor IPP by coordinating to nonbridging oxygens in the diphosphate moiety and residues in the protein. Our data support the latter role for the divalent metal required by the type II enzyme. A comparison of $K_{\text{D}}^{\text{IPP}}$ for type II isomerase in the presence ($4.4 \pm 0.4 \mu\text{M}$) and absence ($84 \pm 9 \mu\text{M}$) of MgCl_2 demonstrates that the metal enhances substrate binding. The dissociation constant for binding of IPP to the enzyme•FMN enzyme in buffer containing Mg^{2+} is similar to $K_{\text{M}}^{\text{IPP}}$ determined from steady state kinetic assays. Thus, it appears that the oxidation state of the cofactor is not important for IPP binding.

When IPP binds, the UV–visible absorbance spectrum of the cofactor changes to one characteristic of neutral reduced flavin, indicating that the reduced flavin anion in the enzyme• FMNH^- complex is protonated. Thus, the catalytically active form of the type II isomerase appears to be an enzyme• FMNH_2 •IPP complex. The pK_{a} of reduced FMN in solution is 6.7 (40). Spectral changes associated with protonation of the enzyme• FMNH^- complex were not observed in the pH range of 6–10. However, observed changes in the presence of IPP over this range suggest a pK_{a} near 8 for the enzyme• FMNH_2 •IPP complex.

A second consequence of IPP binding is the accumulation of a neutral semiquinone during reduction and reoxidation of the enzyme-bound flavin, whose nature was established by UV and EPR experiments. Photoreduction of flavoenzymes with free flavin as a catalyst is thought to occur by both one- and two-electron transfers from reduced free flavin to the enzyme-bound cofactor (31). Our inability to photoreduce flavin in the enzyme•FMN•IPP complex beyond the neutral semiquinone state suggests that the $\text{FMNH}/\text{FMNH}^-$ redox potential in the enzyme•FMN•IPP complex is substantially altered relative to that of free flavin. The neutral semiquinone also forms during reoxidation of the

enzyme•FMNH₂•IPP complex by molecular oxygen, a process that proceeds through sequential one-electron transfers (30, 41). Accumulation of semiquinone during photoreduction and/or reoxidation as the result of a shift in the FMNH[•] (or FMNH₂)/FMNH[•] redox potential has also been observed for flavodoxin (22, 31). Direct participation of IPP in the flavin reduction and oxidation processes is unlikely, given the similar results seen for IPP and the fully saturated analogue isopentyl diphosphate. The measured midpoint redox potentials in the presence of IPP indicate that the accumulation of the neutral semiquinone is derived at least in part from thermodynamic stabilization of the flavin radical state. We have also observed the accumulation of the anionic semiquinone during dithionite titrations without substrate in the presence of either benzyl viologen or indigo carmine as mediators (unpublished results). Thus, the enzyme binds flavin in a manner that thermodynamically stabilizes the semiquinone state.

Three different mechanisms, with different roles for the flavin cofactor, have been suggested for the reaction catalyzed by type II IPP isomerase (Scheme 2). A hydrogen atom addition–abstraction mechanism was originally suggested by Bornemann (17) and later by Hemmi and co-workers (16), on the basis of the observation that reduced flavin was required for catalysis and that apoenzyme reconstituted with 5-deazaFMN, an analogue that only participates in two-electron transfer reactions, was inactive. The initial step would generate a flavin semiquinone–IPP radical pair, followed by hydrogen atom abstraction to give DMAPP and regenerate FMNH₂. This mechanism requires the transient one-electron oxidation of the flavin cofactor. We find that the semiquinone state is stabilized by the enzyme. However, related behavior has been reported for flavoenzymes that do not employ a radical mechanism (42, 43). The second possibility, a hydrogen atom abstraction–addition mechanism with an intermediate allylic radical, seems unlikely. This mechanism involves a transient one-electron reduction of the cofactor, which is not consistent with isomerase•FMNH₂•IPP complex being the catalytically active complex. A third possibility is a protonation–deprotonation mechanism similar to the isomerization catalyzed by the type I enzyme. In this case, FMNH₂ could passively serve in a structural role (17) or could actively participate by protonating the double bond in IPP with a concomitant transient two-electron oxidation of the cofactor. A protonation–deprotonation mechanism was most recently suggested by Hoshino and co-workers (44), following the discovery that an epoxide analogue of IPP, a potent mechanism-based inhibitor of type I IPP isomerase (45), covalently inactivated the type II enzyme. However, it is not clear that the mechanisms for inactivation of the two proteins by the epoxide are similar. We found that NIPP, a potent transition state analogue for the type I enzyme, is a modest inhibitor for type II isomerase.

A protonation–deprotonation mechanism that actively involves the flavin cofactor might use the zwitterionic 5,5-tautomer of FMNH₂ to protonate the double bond in IPP. The 5,5-zwitterion was recently implicated in acid/base chemistry during catalysis (46), and its involvement is consistent with the inability of 5-deazaFMN to substitute for FMN (16). The UV–visible spectrum of a 5,5-dimethyl analogue of the 5,5-FMN tautomer has a peak at ~310–320 nm (47). We see a shoulder near 320 nm in the spectrum

of the isomerase•FMNH₂•IPP complex, although a peak at this wavelength was also reported for the 1,5-tautomer bound to thioredoxin reductase (25, 34). It is interesting to note that the reduction potential for the *tert*-butyl cation in a polar solvent is 90 mV (48). Thus, the redox potential (–196 mV) we measured for oxidation of the enzyme•FMNH₂/FMNH[•]•IPP complex to the enzyme•FMNH[•]•IPP complex suggests that an FMNH[•]•IPPH⁺ ion pair produced by protonation of the double bond in IPP might be unstable with respect to a FMNH[•]•IPPH[•] radical pair, unless it is selectively stabilized by the enzyme. Otherwise, one would anticipate that at some point along a putative protonation reaction coordinate an electron transfer would generate the radical pair. At this point, additional work is needed to convincingly resolve the mechanism of reaction catalyzed by type II IPP isomerase.

ACKNOWLEDGMENT

We thank Dr. Wenyun Gao and Nicole Heaps for samples of DMAPP. We also thank Professor Ann Walker and Dr. Andrie Astashkin for assistance with EPR spectroscopy, Dr. Elliot Rachlin for assistance with mass spectrometry, and Professor Vahe Bandarian for assistance with anaerobic experiments and helpful discussions.

SUPPORTING INFORMATION AVAILABLE

Fluorescence of the guanidinium-released flavin and for binding of oxidized enzyme•FMN to IPP as measured via ultrafiltration assays, figures and experimental details for the dependence of isomerase activity on exogenous FMN and for enzyme inhibition by NIPP and isopentyl diphosphate, anaerobic spectra of the dithionite-reduced enzyme, spectra for aerobic reduction of the enzyme by NADPH and reoxidation of the photoreduced enzyme, EPR spectra of enzyme•FMNH[•] complexes, and UV–visible spectra of reductive potentiometric titrations. This material is available free of charge via the Internet at <http://pubs.acs.org>.

REFERENCES

1. Rohdich, F., Bacher, A., and Eisenreich, W. (2004) Perspectives in anti-infective drug design. The late steps in the biosynthesis of the universal terpenoid precursors, isopentenyl diphosphate and dimethylallyl diphosphate, *Bioorg. Chem.* 32, 292–308.
2. Kuzuyama, T., and Seto, H. (2003) Diversity of the biosynthesis of the isoprene units, *Nat. Prod. Rep.* 20, 171–183.
3. Rohmer, M. (1999) A mevalonate-independent route to isopentenyl diphosphate, in *Comprehensive Natural Products Chemistry* (Cane, D., Ed.) pp 45–67, Pergamon Press, New York.
4. Laupitz, R., Hecht, S., Amslinger, S., Zepeck, F., Kaiser, J., Richter, G., Schramek, N., Steinbacher, S., Huber, R., Arigoni, D., Bacher, A., Eisenreich, W., and Rohdich, F. (2004) Biochemical characterization of *Bacillus subtilis* type II isopentenyl diphosphate isomerase, and phylogenetic distribution of isoprenoid biosynthesis pathways, *Eur. J. Biochem.* 271, 2658–2669.
5. Agranoff, B. W., Eggerer, H., Henning, U., and Lynen, F. (1959) Isopentenyl pyrophosphate isomerase, *J. Am. Chem. Soc.* 81, 1254–1255.
6. Lee, S., and Poulter, C. D. (2006) *Escherichia coli* Type I Isopentenyl Diphosphate Isomerase: Structural and Catalytic Roles for Divalent Metals, *J. Am. Chem. Soc.* 128, 11545–11550.
7. Cornforth, J. W., Cornforth, R. H., Popjak, G., and Yengoyan, L. (1966) Studies on the biosynthesis of cholesterol. XX. Steric course of decarboxylation of 5-pyrophosphomevalonate and of the carbon to carbon bond formation in the biosynthesis of farnesyl pyrophosphate, *J. Biol. Chem.* 241, 3970–3987.
8. Cornforth, J. W., and Popjak, G. (1969) Chemical syntheses of substrates of sterol biosynthesis, *Methods Enzymol.*, 359–371.

9. Clifford, K. H., Cornforth, J. W., Mallaby, R., and Phillips, G. T. (1971) Stereochemistry of isopentenyl pyrophosphate isomerase, *J. Chem. Soc. D*, 1599–1600.
10. Muehlbacher, M., and Poulter, C. D. (1988) Isopentenyl-diphosphate isomerase: Inactivation of the enzyme with active-site-directed irreversible inhibitors and transition-state analogues, *Biochemistry* 27, 7315–7328.
11. Reardon, J. E., and Abeles, R. H. (1986) Mechanism of action of isopentenyl pyrophosphate isomerase: Evidence for a carbonium ion intermediate, *Biochemistry* 25, 5609–5616.
12. Durbecq, V., Sainz, G., Oudjama, Y., Clantin, B., Bompard-Gilles, C., Tricot, C., Caillet, J., Stalon, V., Droogmans, L., and Villeret, V. (2001) Crystal structure of isopentenyl diphosphate:dimethylallyl diphosphate isomerase, *EMBO J.* 20, 1530–1537.
13. Wouters, J., Oudjama, Y., Ghosh, S., Stalon, V., Droogmans, L., and Oldfield, E. (2003) Structure and mechanism of action of isopentenylpyrophosphate-dimethylallylpyrophosphate isomerase, *J. Am. Chem. Soc.* 125, 3198–3199.
14. Wouters, J., Oudjama, Y., Barkley, S. J., Tricot, C., Stalon, V., Droogmans, L., and Poulter, C. D. (2003) Catalytic mechanism of *Escherichia coli* isopentenyl diphosphate isomerase involves Cys-67, Glu-116, and Tyr-104 as suggested by crystal structures of complexes with transition state analogues and irreversible inhibitors, *J. Biol. Chem.* 278, 11903–11908.
15. Kaneda, K., Kuzuyama, T., Takagi, M., Hayakawa, Y., and Seto, H. (2001) An unusual isopentenyl diphosphate isomerase found in the mevalonate pathway gene cluster from *Streptomyces* sp. strain CL190, *Proc. Natl. Acad. Sci. U.S.A.* 98, 932–937.
16. Hemmi, H., Ikeda, Y., Yamashita, S., Nakayama, T., and Nishino, T. (2004) Catalytic mechanism of type 2 isopentenyl diphosphate: dimethylallyl diphosphate isomerase: Verification of a redox role of the flavin cofactor in a reaction with no net redox change, *Biochem. Biophys. Res. Commun.* 322, 905–910.
17. Bornemann, S. (2002) Flavoenzymes that catalyze reactions with no net redox change, *Nat. Prod. Rep.* 19, 761–772.
18. Davisson, V. J., Woodside, A. B., and Poulter, C. D. (1985) Synthesis of allylic and homoallylic isoprenoid pyrophosphates, *Methods Enzymol.* 110, 130–144.
19. de Ruyck, J., Rothman, S. C., Poulter, C. D., and Wouters, J. (2005) Structure of *Thermus thermophilus* type 2 isopentenyl diphosphate isomerase inferred from crystallography and molecular dynamics, *Biochem. Biophys. Res. Commun.* 338, 1515–1518.
20. Satterwhite, D. M. (1985) Isopentenyl diphosphate δ -isomerase, *Methods Enzymol.* 110, 92–99.
21. Copeland, R. A. (2000) *Enzymes: A Practical Introduction to Structure, Mechanism, and Data Analysis*, Wiley-VCH, New York.
22. Yalloway, G. N., Mayhew, S. G., Malthouse, J. P., Gallagher, M. E., and Curley, G. P. (1999) pH-dependent spectroscopic changes associated with the hydroquinone of FMN in flavodoxins, *Biochemistry* 38, 3753–3762.
23. Murataliev, M. B. (1999) Application of electron spin resonance (ESR) for detection and characterization of flavoprotein semiquinones, *Methods Mol. Biol.* 131, 97–110.
24. Dutton, P. L. (1978) Redox potentiometry: Determination of midpoint potentials of oxidation-reduction components of biological electron-transfer systems, *Methods Enzymol.* 54, 411–435.
25. Ghisla, S., Massey, V., Lhoste, J. M., and Mayhew, S. G. (1974) Fluorescence and optical characteristics of reduced flavines and flavoproteins, *Biochemistry* 13, 589–597.
26. Barkley, S. J., Cornish, R. M., and Poulter, C. D. (2004) Identification of an Archaeal type II isopentenyl diphosphate isomerase in *Methanothermobacter thermautotrophicus*, *J. Bacteriol.* 186, 1811–1817.
27. Barkley, S. J., Desai, S. B., and Poulter, C. D. (2004) Type II isopentenyl diphosphate isomerase from *Synechocystis* sp. strain PCC 6803, *J. Bacteriol.* 186, 8156–8158.
28. Takagi, M., Kaneda, K., Shimizu, T., Hayakawa, Y., Seto, H., and Kuzuyama, T. (2004) *Bacillus subtilis* ypgA gene is fni, a nonessential gene encoding type 2 isopentenyl diphosphate isomerase, *Biosci., Biotechnol., Biochem.* 68, 132–137.
29. Yamashita, S., Hemmi, H., Ikeda, Y., Nakayama, T., and Nishino, T. (2004) Type 2 isopentenyl diphosphate isomerase from a thermoacidophilic archaeon *Sulfolobus shibatae*, *Eur. J. Biochem.* 271, 1087–1093.
30. Massey, V. (2000) The chemical and biological versatility of riboflavin, *Biochem. Soc. Trans.* 28, 283–296.
31. Massey, V., Stankovich, M., and Hemmerich, P. (1978) Light-mediated reduction of flavoproteins with flavins as catalysts, *Biochemistry* 17, 1–8.
32. Massey, V., and Hemmerich, P. (1978) Photoreduction of flavoproteins and other biological compounds catalyzed by deazaflavins, *Biochemistry* 17, 9–16.
33. Müller, F. (1992) Nuclear magnetic resonance studies on flavoproteins, in *Chemistry and Biochemistry of Flavoenzymes* (Müller, F., Ed.) pp 557–595, CRC Press, Boca Raton, FL.
34. Eisenreich, W., Kemter, K., Bacher, A., Mulrooney, S. B., Williams, C. H., Jr., and Muller, F. (2004) ^{13}C -, ^{15}N - and ^{31}P -NMR studies of oxidized and reduced low molecular mass thioredoxin reductase and some mutant proteins, *Eur. J. Biochem.* 271, 1437–1452.
35. Ghisla, S. (1980) Fluorescence and optical characteristics of reduced flavins and flavoproteins, *Methods Enzymol.* 66, 360–373.
36. Massey, V., and Palmer, G. (1966) On the existence of spectrally distinct classes of flavoprotein semiquinones. A new method for the quantitative production of flavoprotein semiquinones, *Biochemistry* 5, 3181–3189.
37. Kay, C. M. W., and Weber, S. (2002) EPR of radical intermediates in flavoenzymes, in *Electron Paramagnetic Resonance* (Gilbert, B. C., Davies, M. J., and Murphy, D. M., Eds.) pp 222–253, Royal Society of Chemistry, London.
38. Mayhew, S. G. (1999) The effects of pH and semiquinone formation on the oxidation-reduction potentials of flavin mononucleotide. A reappraisal, *Eur. J. Biochem.* 265, 698–702.
39. Steinbacher, S., Kaiser, J., Gerhardt, S., Eisenreich, W., Huber, R., Bacher, A., and Rohdich, F. (2003) Crystal structure of the type II isopentenyl diphosphate: Dimethylallyl diphosphate isomerase from *Bacillus subtilis*, *J. Mol. Biol.* 329, 973–982.
40. Draper, R. D., and Ingraham, L. L. (1968) A potentiometric study of the flavin semiquinone equilibrium, *Arch. Biochem. Biophys.* 125, 802–808.
41. Eberlein, G., and Bruce, T. C. (1982) One and two electron reduction of oxygen by 1,5-dihydroflavins, *J. Am. Chem. Soc.* 104, 1449–1452.
42. Gadda, G., and Fitzpatrick, P. F. (1998) Biochemical and physical characterization of the active FAD-containing form of nitroalkane oxidase from *Fusarium oxysporum*, *Biochemistry* 37, 6154–6164.
43. Fullerton, S. W., Daff, S., Sanders, D. A., Ingledew, W. J., Whitfield, C., Chapman, S. K., and Naismith, J. H. (2003) Potentiometric analysis of UDP-galactopyranose mutase: Stabilization of the flavosemiquinone by substrate, *Biochemistry* 42, 2104–2109.
44. Hoshino, T., Tamegai, H., Kakinuma, K., and Eguchi, T. (2006) Inhibition of type 2 isopentenyl diphosphate isomerase from *Methanocaldococcus jannaschii* by a mechanism-based inhibitor of type 1 isopentenyl diphosphate isomerase, *Bioorg. Med. Chem.* (in press).
45. Lu, X. J., Christensen, D. J., and Poulter, C. D. (1992) Isopentenyl-diphosphate isomerase: Irreversible inhibition by 3-methyl-3,4-epoxybutyl diphosphate, *Biochemistry* 31, 9955–9960.
46. Macheroux, P., Ghisla, S., Sanner, C., Ruterjans, H., and Muller, F. (2005) Reduced flavin: NMR investigation of N5-H exchange mechanism, estimation of ionisation constants and assessment of properties as biological catalyst, *BMC Biochem.* 6, 26.
47. Ghisla, S., Hartmann, U., Hemmerich, P., and Müller, F. (1973) Die reduktive Alkylierung des Flavinkerns 2; Struktur und Reaktivität von Dihydroflavinen, *Liebigs Ann. Chem.* 8, 1388–1415.
48. Wayner, D. D. M., McPhee, D. J., and Griller, D. (1988) Oxidation and reduction potentials of transient free radicals, *J. Am. Chem. Soc.* 110, 132–137.

BI0616347